Scientific
Research
Publishing

Unique Pulsed-Laser Deposition Production of Anatase and Rutile TiO$_2$ on Al$_2$O$_3$

Alexandra Gordienko[1], Anthony B. Kaye[1,2]

[1]Department of Physics and the Nano Tech Center, Texas Tech University, Lubbock, Texas, USA
[2]United States Air Force Nuclear Weapons Center, 1551 Wyoming Blvd., Kirtland Air Force Base, New Mexico, USA
Email: alex.gordienko@ttu.edu, anthony.kaye.1@us.af.mil

Abstract

Two pure hexagonal phases of titanium dioxide, anatase and rutile, were grown on c-cut Al$_2$O$_3$ substrates via pulsed-laser deposition by changing only the growth and annealing conditions, but without changing the substrate, target, or working gas. Purity of each phase was confirmed by x-ray diffraction, the quality of each film was studied using atomic force microscopy and scanning electron microscopy, and the interface between each substrate and film was studied using x-ray photoelectron spectroscopy. A binding layer of Ti$_2$O$_3$ was found to explain anatase growth under the very large lattice mismatch conditions.

Keywords

Titania, Anatase, Rutile, Sapphire, PLD

1. Introduction

Titanium dioxide (titania; TiO$_2$) is a well-studied material that has been studied since at least 1916 [1]. Titania has a number of properties that make it useful for a wide variety of applications; these include using TiO$_2$ as the basis for energy efficient solar cells [2] [3], as photocatalytic materials to clean air and water [4] [5] [6], for self-cleaning coatings [7], as components of various sensor devices [8] [9] [10], and as a gate dielectric in MOSFET technologies [11] [12] [13]. Further, because it is a wide bandgap semiconductor, titanium dioxide is becoming increasingly important for many next-generation modern optical and electronics applications, such as transparent electronics systems, transparent thin-film transistors, and see-through active matrix displays. The success of each of these applications depends critically upon the particular crystallographic state (anatase,

rutile, or brookite) of the titania being utilized (see, e.g., Park *et al.* [3], Gÿorgy *et al.* [10], Kim *et al.* [13], and Luttrell *et al.* [5]).

Over the last 100 years, a wide variety of methods have been developed to produce titania, each method optimized for the final form of titania required. Methodologies that are currently employed to produce bulk TiO_2 include solid state reactions [2] [4] [14] and sol-gel methods [9] [15]; however, generally speaking, there are a wider variety of thin-film production techniques used for titania, including reactive sputtering [16], spray pyrolysis [17], sol-gel techniques [13] [18], chemical vapor deposition [19], and pulsed-laser deposition (PLD; [5] [6] [20]-[28]).

While each of these growth techniques has its advantages and disadvantages, PLD is one of the most common, forming the basis of more than 100 publications over the last ten years. However, when searching this literature for PLD growth protocols for specific crystallographic phases, a clear pattern emerged: researchers tended to favor using a pure titanium target with a silicon substrate to grow anatase titania (see, e.g., Di Fonzo *et al.* [4], Luca *et al.* [20], and Gÿorgy *et al.* [21]), whereas typical growth protocols for rutile thin films used rutile titania targets and either glass or silicon substrates (see, e.g., Gÿorgy *et al.* [21], Dzibrou *et al.* [24], and Long *et al.* [25]). Kitazawa *et al.* [26], Luttrell *et al.* [5] and Le Boulbar *et al.* [27] used c-cut Al_2O_3 as their substrate for growing rutile TiO_2, but in every instance in which researchers used Al_2O_3 as a substrate, it was switched for $LaAlO_3$ when they attempted to produce anatase TiO_2. According to Luca *et al.* [20], Janisch *et al.* [29], and references therein, growing TiO_2 on Al_2O_3 leads to either rutile, mixed-phase films or brookite films. For studies that considered multiple distinct crystallographic forms, researchers changed either the PLD target (see, e.g., Hsieh *et al.* [22] and Ohshima *et al.* [23]) or the substrate (see, e.g., Luttrell *et al.* [5], Kitazawa *et al.* [26], and Le Boulbar *et al.* [27]) to achieve their goal.

Further, there is no prior report of the production of anatase TiO_2 on Al_2O_3. We note, however, that some authors (see, e.g., Murugesan *et al.* [30], Djerdj and Tonejc [31]) call titania films "anatase" when anatase is the dominant phase in mixed-phase films. This may be done because it has been suggested that pure anatase cannot be grown on sapphire substrates (Luca *et al.* [20]).

In this paper, we show that both pure anatase and rutile phases of TiO_2 can be individually grown using a single PLD target and a single substrate material (c-cut Al_2O_3) by carefully controlling the growth and annealing conditions. Understanding how to produce given phases of a material using a single PLD target and a single substrate is vital for both understanding the growth physics of the material and for large-scale manufacturing, since changing growth materials can make it difficult to determine correlations between growth conditions and the performance of the resulting film. Such ambiguity may be at least one reason why different research groups found vastly different growth parameters to be ideal for the same TiO_2 crystallographic phase (cf. Hsieh *et al.* [22], Dzibrou *et al.* [24], Long *et al.* [25], and Choi *et al.* [28]).

2. Experimental Section

We grew thin films using custom-built pulsed-laser deposition system (shown in Figure 1) with a Coherent COMPex Pro KrF excimer laser (λ = 256 nm, pulse width = 25 ns) held at a 45° angle to a rotating TiO_2 mixed-phase target inside a custom-built growth chamber (total volume = 35 L) with a base pressure of 6.5×10^{-11} Torr. The thin film growth process was typically started near pressure of ~2 $\times 10^{-9}$ Torr. The target was 1-in. in diameter, 0.25-in. thick, and 99.99% pure (SuperConductor Materials). To ensure even ablation, the target was rotated at ~3 rpm. In every case, we grew the film on a 10 mm × 10 mm c-cut (0001) Al_2O_3 substrate that was heated from back side with a platinum wire heater; temperature was measured with a thermocouple placed in a representative position, and the substrate was rotated parallel to, but in an opposite direction from the target at ~3 rpm during the entire deposition process.

Anatase films were annealed inside the growth chamber; the film was held at its growth temperature and pressure for one hour and then allowed to cool at a rate of ~9°C/min. until it reached room temperature. Rutile films were annealed in a custom-built quartz-tube furnace (base pressure of ~1×10^{-4} Torr). To ensure that the films did not crack, they were inserted into the furnace at room temperature and returned to the temperature and pressure at which they were grown with a ramp rate of 9°C/min; after 1 hour for anatase and 2 hours for rutile films, the films were returned to room temperature with a −9°C/min cooling ramp rate.

Finally, film thicknesses were measured by imaging a cross section of each sample with a Zeiss Crossbeam 340 focused ion-beam/scanning-electron microscope.
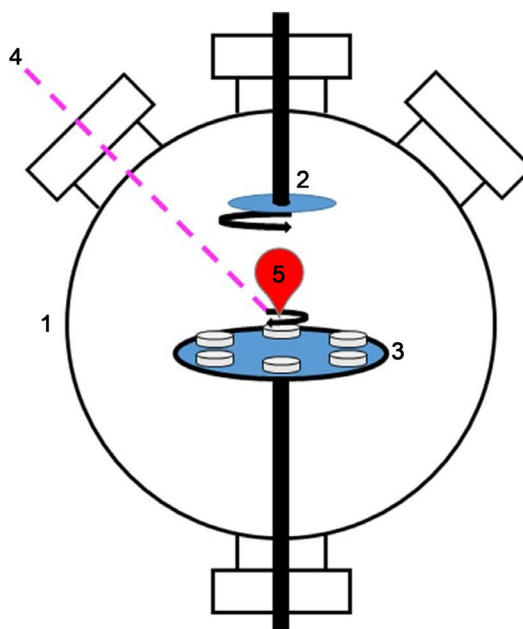

Figure 1. Schematic representation of the PLD system used for sample deposition. Numbered labels correspond to: 1: Ultra High Vacuum chamber; 2: rotatable substrate holder; 3: rotatable target holders; 4: incident UV laser beam; and 5: material plume.

The specific growth and annealing protocols required to produce each film are presented in Table 1; using these protocols, films ranging from tens of nm to up to 1.5 μm were created by changing only the number of laser pulses. Anatase films grew at 0.1Å per laser pulse (5Å per second); rutile films grew three times faster.

After production, each film was analyzed using a Rigaku Ultima 3 powder x-ray diffraction (XRD) system to inspect quality of the films in terms of crystallographic phase and crystallinity. The samples were measured from 20° to 85° (2θ) with a step size of 0.02° and an integration time of 0.6 s per step.

To measure the roughness, representative films were measured with an Asylum Research MFP-3D-BIO atomic force microscope (AFM) in tapping mode with Bruker MSNL probes (nominal tip radii of 2 nm) to characterize the surface morphology of each sample. Individual locations on each sample for a 10 μm × 10 μm scan were selected near the center of each sample to minimize edge effects. For each scan, the rate was set to 0.5 Hz, the scan angle was fixed at 90°, the set point was held at 1 V, and the integral gain was set to 10.

To study the interface between the films and substrate, we used x-ray photoelectron spectroscopy (XPS). Each film was produced by the protocol described above, but changing the number of laser pulses to 200 for rutile films and 600 for anatase films in order to produce films that were ~6 nm thick. XPS measurements were completed using a Physical Electronics PHI 5000 Versa Probe spectrometer using a monochromatic Al Kα ($h\nu$ = 1486.6 eV) x-ray source. Peaks

Table 1. TiO$_2$ film growth conditions.

Condition	1	2
Laser Settings		
Pulse energy (mJ)	296	222
Repetition rate (Hz)	50	5
Fluence (J·cm^{-2})	2.0	1.5
Number of shots	10,000[a]	3,000[b]
Growth Conditions		
Chamber pressure (mTorr)	35	5
Background gas	O$_2$	O$_2$
Substrate temperature (°C)	250	700
Target-to-substrate distance (mm)	65	60
Annealing Conditions		
Pressure (mTorr)	35	5
Background gas	O$_2$	O$_2$
Temperature (°C)	250	900
Time (hr)	1	2

[a]Corresponding film thickness: 100 nm; [b]Corresponding film thickness: 90 nm.

reported were charge corrected using the adventitious carbon 1s peak at 284.5 eV as a reference.

3. Results and Discussion

We show the x-ray diffraction patterns in **Figure 2**, in which the rutile and anatase patterns are on the top (red) and bottom (blue), respectively. The rutile pattern has been shifted vertically for visual clarity; patterns were identified with the JadeTM software package. The anatase phase matched with PDF#97-015-460431 and the rutile phase matched with PDF#03-065-1119; [32] each peak is labeled with its corresponding Miller index from the corresponding matching file.

Note that both plots are clean; there are no anatase peaks in the rutile pattern and vice versa. The peak labeled with a red dagger (†) in the top panel is a reflection from the Inconel sample holder and is not part of the film.

Since the XRD patterns of anatase and brookite are very similar, we must be cautious when claiming that we have pure anatase phase TiO_2. To aid in this, we note that in the anatase pattern in **Figure 2** (the lower, blue curve), there is no peak near 30.81˚ (the location of the (121) reflection of brookite), and there is a peak at 62.67˚, corresponding to the (024) reflection of anatase. The combination of these two facts are sufficient to claim that our anatase is brookite-free (Di Paola *et al.* [33] and Hu *et al.* [34].

Substrate effects

The main conditions required to produce strain-free epitaxial film growth are (a) a thermal match between the film and the substrate and (b) matched crystallographic lattice structures. Mismatches in either result in films that have residual stress and potential lattice defects that may alter the performance of the final film. [35] Therefore, the choice of substrate is critical when growing any kind
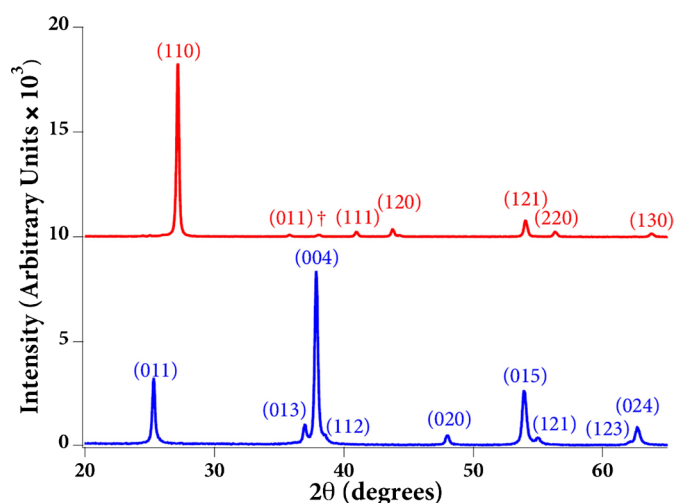

Figure 2. X-ray diffraction patterns for the rutile (top, red) and anatase (bottom, blue) samples. Miller indices for each reflection matching PDF#03-065-111932 (for the rutile pattern) and PDF#97-015-460431 (for the anatase pattern) are shown for each visible peak. The peak labeled by a red dagger (†) symbol in the top panel is a reflection from the sample holder and is not part of the film; see text for details.

of thin film, and especially those with multiple crystallographic forms (e.g., TiO_2). To investigate how potential mismatches may affect the growth of anatase and rutile TiO_2, we generated Table 2, below. In Table 2, for every substrate material listed in column 1, we provide a room-temperature value of the lattice constant a in column 2, and then compute a temperature-adjusted lattice mismatch ε as:

$$\varepsilon = \frac{a_f - a_s}{a_s},$$
(1)

in which the subscripts f, and s stand for "film," and "substrate," respectively, and in which the individual lattice constants are computed at the growth temperature indicated in Table 1 for anatase (250°C; column 3) and rutile (700°C; column 4) TiO_2. The lattice mismatch values assume room-temperature TiO_2 lattice constants of 3.7852 and 4.5933 A, respectively. [36] Lastly, we considered that since it is increasingly difficult to find external funding, substrate cost may be a factor in decision-making, so we provide the approximate cost of each substrate in USD/cm^2 the last column of Table 2.

Anatase films

The anatase sample was both grown and annealed at 250°C. This low growth temperature, combined with the significantly higher oxygen partial pressure resulted in a film that grew relatively slowly (having growth rate of 0.1 Å per pulse, or 5 Å per second). The sample is transparent, and has an rms roughness < 1 nm (for reference, the typical roughness of the c-cut Al_2O_3 substrates was measured to be 0.098 nm). The bottom panel of Figure 2 shows that the XRD pattern of this sample is clean, showing only anatase peaks; the large peak at 38.014° indicates that our anatase sample has a preferred orientation in the (004) plane.

It is apparent from Table 2 why many researchers producing anatase TiO_2 would select $LaSrAlO_4$ and $SrTiO_3$ as their substrates. However, these represent two of the three most expensive substrates on our list; the third best lattice

Table 2. Comparing crystallographic properties of typically-used substrates to TiO_2.

Substrate Material	a (A)	ε (Anatase) (%)	ε (Rutile) (%)	Approx. Cost[a] (USD/cm^2)
Al_2O_3	4.759213[b]	20.54[c]	3.51	2.17
GaAs	5.65325[d]	33.09[d]	18.69	13.28
$LaAlO_3$	5.3646[e]	29.51[e]	21.01	14.22
$LaSrAlO_4$	3.75664[f]	0.61[f]	22.19	129.00
Si	5.4307[g]	30.31[h]	15.19	2.30
SiO_2	4.912[i]	23.20[i]	7.56	3.19
$SrTiO_3$	3.905268[j]	3.72[k]	15.74	119.80
Ti	2.95111[l]	28.08[m]	55.51	45.01

[a]Substrate costs were estimated from the MTI Corp. online catalog at mitxtl.com on 22 June 2018; [b]Dobrovinskaya *et al.* [37]; [c]Reeber and Wang [38]; [d]Blakemore [39]; [e]Howard *et al.* [40]; [f]Kawamura *et al.* [41]; [g]Hössinger [42]; [h]Watanabe *et al.* [43]; [i]Ackermann and Sorrell [44]; [j]Schmidbauer *et al.* [45]; [k]de Ligny and Richet [46]; [l]Wood [47]; [m]Spreadborough and Christian [48].

match in Table 2 is Al$_2$O$_3$, which is available at a significantly lower cost. We also note that SrTiO$_3$ can be grown in the (100) orientation as an atomically flat buffer layer in which the entire surface is terminated at the TiO$_2$ layer, [49] [50] leading to a virtually perfect match between the buffer layer and the film. In fact, both SrTiO$_3$ and LaAlO$_3$ have been shown to be excellent substrates for both anatase and rutile TiO$_2$ (see, e.g., Kennedy and Stampe [51]), but under conditions significantly different from ours (e.g., LaAlO$_3$ was used at temperatures above its phase change, occurring at ~820 K). Such excellent crystallographic matches under the conditions described by Kennedy and Stampe [51] also explain why SrTiO$_3$ is used as a substrate for TiO$_2$. However, these spectacular crystallographic matches come both at considerable cost and require a relatively complex growth protocols to obtain both phases of titania on the same substrate. For example, Hsieh *et al.* obtained both anatase and rutile TiO$_2$ on SrTiO$_3$ substrates, but while the anatase phase was deposited directly on the substrate, the rutile phase was grown by oxidizing titanium nitride films [22].

One of the most interesting discoveries we made was determining how anatase titania films could be grown so easily on sapphire substrates given the very large lattice mismatch. We used XPS to study the interface physics between our c-cut sapphire substrate and film.

The high resolution Ti(2p) spectrum shown in Figure 3 (black curve) was deconvolved into four individual curves: the peaks labeled A (at 459.0 eV; red curve) and B (at 464.6 eV; green curve) represent the 2p3/2 and 2p1/2 energy levels of TiO$_2$, respectively. Similarly, the peaks labeled C (at 457.8 eV; magenta curve) and D (at 462.0 eV; blue curve) correspond to the 2p3/2 and 2p1/2 energy levels of Ti$_2$O$_3$. These results indicate that a thin layer of Ti$_2$O$_3$ was observed using XPS. Ti$_2$O$_3$ has hexagonal lattice structure with nearly identical to Al$_2$O$_3$ lattice parameters. When the upper layer of sapphire is the oxygen-saturated layer, titanium atoms can be deposited in such a way that the resulting structure is the
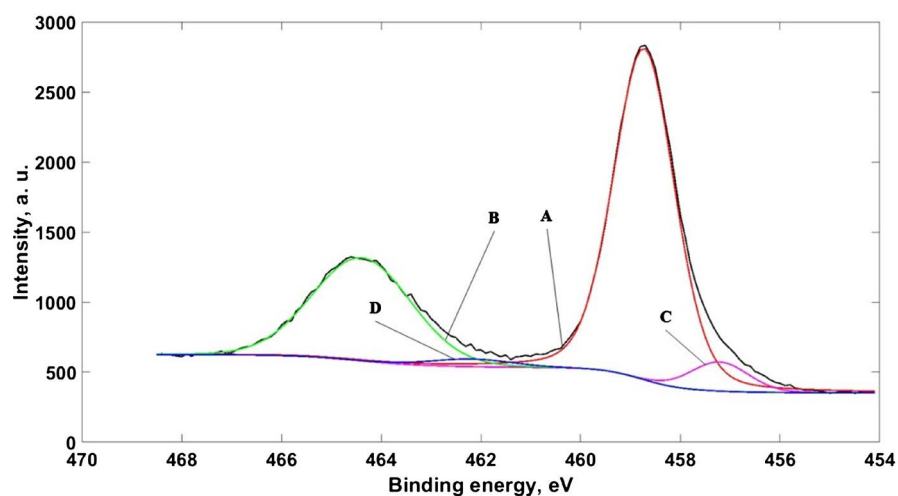

Figure 3. X-ray photoelectron spectroscopy results for anatase film. Peaks corresponding to binding energies of 2p3/2 and 2p1/2 of TiO$_2$ are labeled A and B. Peaks corresponding to binding energies of 2p3/2 and 2p1/2 of Ti$_2$O$_3$ are labeled C and D.

exact replication of Al_2O_3 structure. Therefore, a thin binding layer of Ti_2O_3 is formed on sapphire surface during anatase film deposition to allow matching the sapphire crystal to anatase structure. Further anatase TiO_2 growth becomes energetically more efficient compared to growth on sapphire, since the binding energy of direct Ti-Ti bond (117.6 kJ/mol (Luo [52])) is lower than binding energy of direct Ti-Al bond (263.4 kJ/mol (Luo [52])). Ti_2O_3 layer is thin enough so it is not visible in XRD scans presented in **Figure 2**, but has a large enough effect to mitigate the lattice mismatch in growing anatase films with virtually zero strain.

Rutile films

We confirm the results of Gouma and Mills [53], who have shown that the rutile phase is preferred when films are grown and annealed at higher temperatures compared to those required for the growth of anatase films. Our rutile film grew at 0.3 Å per pulse (or 1.5 Å per second), appears to be clear and smooth, and has an rms roughness of <1 nm.

In the top panel of **Figure 2**, we can see that the XRD pattern of this sample only contains peaks for rutile phase of titania, except for one small peak near 38.5˚. This anomalous peak matches the XRD pattern of the Inconel sample holder used in these experiments, and are not part of the film. The sample has preferred orientation in (110) plane as evidenced by the very large peak at 27.432˚; this explains why one of the possible rutile peaks in our range (the (020) peak at 39.185˚) is not present.

Similar to the anatase samples (above), we were above to deconvolve a single high-resolution XPS spectrum (black curve) into three individual peaks. In **Figure 4**, the peaks labeled A (at 459.1 eV; red curve) and B (at 464.8 eV; green curve) represent the 2p1/2 and 2p3/2 energy levels of TiO_2, respectively. The peak labeled C (at 460.1 eV; blue curve) represents the 2p1/2 energy level of TiO.
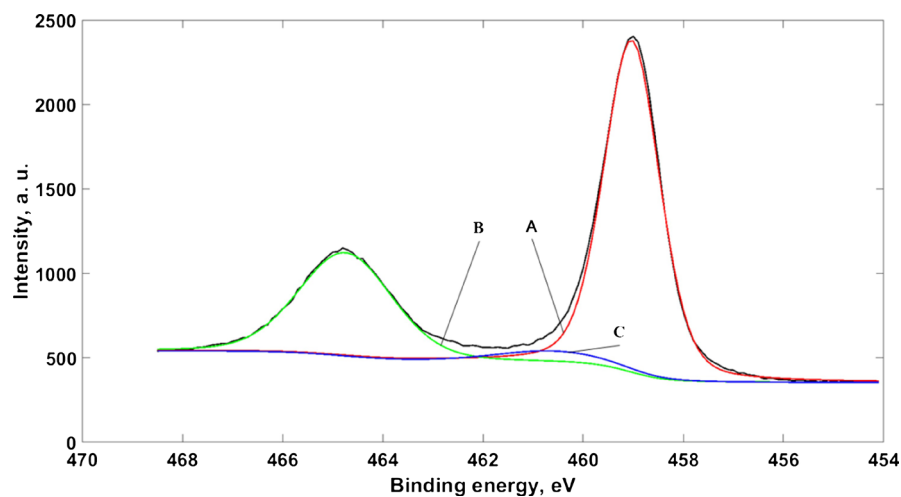

Figure 4. High-resolution x-ray photoelectron spectroscopy results for a typical rutile film. Peaks corresponding to binding energies of 2p3/2 and 2p1/2 of TiO_2 are labeled A and B (red and green curves, respectively). The single small peak corresponding to the 2p1/2 binding energy of TiO is labeled C (blue curve). See text for details.

The very small amplitude of the TiO peak in the deconvolved spectrum suggests that TiO is only present in the film as an deficiency defect at the crystalline interface.

From Table 2, it is clear that Al_2O_3 is one of the most optimal substrates for growing rutile titania, and the literature confirms that it is frequently used for this purpose (see, e.g., Luttrell *et al.* [5], Kitazawa *et al.* [26], and Le Boulbar *et al.* [27]). We note for completeness that an intermediate layer of Ti_2O_3 is not present in the rutile sample, unlike anatase grown sample. This suggests that that the low lattice mismatch between rutile titania and c-cut sapphire doesn't require an intermediate layer at their interface. However, a small amount of TiO is present in the rutile sample, this could be caused by growth and annealing oxygen pressure being slightly below an optimal value for rutile growth.

4. Conclusion

We have shown that the growth of pure rutile and pure anatase TiO_2 is possible without changing substrate materials or PLD targets, and we have done so using only c-cut Al_2O_3 as a substrate—despite the large lattice mismatch between Al_2O_3 and anatase phase of TiO_2. Growing anatase in this manner does, however, induce significantly more strain in the anatase film compared to the rutile film grown on the same substrate. XPS data showed that anatase growth on c-cut sapphire is likely possible, due to the specific PLD growth conditions, to accommodate growth of Ti_2O_3 intermediate layer that binds TiO_2 film with tetragonal lattice structure to hexagonal structure of Al_2O_3, although this conclusion requires additional experimental data to confirm it as the only way anatase can be grown this way. This intermediate layer is not found in our rutile films, however, oxygen vacancy defects were observed by XPS. They are possibly a result of lower oxygen pressure used during growth and annealing of rutile films. In any case, for applications in which titania is used for its optical properties, Al_2O_3 substrates may be a new preferred substrate, both because it could significantly decrease production costs and because of the various material properties of sapphire.

Acknowledgements

Conflicts of Interest

The authors declare no conflicts of interest regarding the publication of this paper.

References

[1] Vegard, L. (1916) Results of Crystal Analysis. *The London, Edinburgh, and Dublin*

Philosophical Magazine and Journal of Science, **32**, 65-96.
https://doi.org/10.1080/14786441608635544

[2] Mincuzzi, G., Vesce, L., Reale, A., Di Carlo, A. and Brown, T.M. (2009) Efficient Sintering of Nanocrystalline Titanium Dioxide Films for Dye Solar Cells via Raster Scanning Laser. *Applied Physics Letters*, **95**, Article ID: 103312.
https://doi.org/10.1063/1.3222915

[3] Park, N.-G., van de Lagemaat, J. and Frank, A.J. (2000) Comparison of Dye-Sensitized Rutile-and Anatase-Based TiO_2 Solar Cells. *Journal of Physical Chemistry B*, **104**, 8989-8994. https://doi.org/10.1063/1.3222915

[4] Di Fonzo, F., Casari, C.S., Russo, V., Brunella, M.F., Bassi, A.L. and Bottani, C.E. (2008) Hierarchically Organized Nanostructured TiO_2 for Photocatalysis Applications. *Nanotechnology*, **20**, Article ID: 015604.
https://doi.org/10.1088/0957-4484/20/1/015604

[5] Luttrell, T., Halpegamage, S., Sutter, E. and Batzill, M. (2014) Photocatalytic Activity of Anatase and Rutile TiO_2 Epitaxial Thin Film Grown by Pulsed Laser Deposition. *Thin Solid Films*, **564**, 146-155. https://doi.org/10.1016/j.tsf.2014.05.058

[6] Lin, H., Rumaiz, A.K., Schulz, M., Wang, D., Rock, R., Huang, C.P. and Shah, S.I. (2008) Photocatalytic Activity of Pulsed Laser Deposited TiO_2 Thin Films. *Materials Science and Engineering B*, **151**, 133-139.
https://doi.org/10.1016/j.mseb.2008.05.016

[7] Roméas, V., Pichat, P., Guillard, C., Chopin, T. and Lehaut, C. (1999) Testing the Efficacy and the Potential Effect on Indoor Air Quality of a Transparent Self-Cleaning TiO_2-Coated Glass through the Degradation of a Fluoranthene Layer. *Industrial & Engineering Chemistry Research*, **38**, 3878-3885.
https://doi.org/10.1021/ie990326k

[8] Bao, S.-J., Li, C.M., Zang, J.-F., Cui, X.-Q., Qiao, Y. and Guo, J. (2008) New Nanostructured TiO_2 for Direct Electrochemistry and Glucose Sensor Applications. *Advanced Functional Materials*, **18**, 591-599. https://doi.org/10.1002/adfm.200700728

[9] Du, X., Wang, Y., Mu, Y., Gui, L., Wang, P. and Tang, Y. (2002) A New Highly Selective H_2 Sensor Based on TiO_2/PtO-Pt Dual-Layer Films. *Chemistry of Materials*, **14**, 3953-3957. https://doi.org/10.1021/cm0201293

[10] Gÿorgy, E., Socol, G., Axente, E., Mihailescu, I.N., Ducu, C. and Ciuca, S. (2005) Anatase Phase TiO_2 Thin Films Obtained by Pulsed Laser Deposition for Gas Sensing Applications. *Applied Surface Science*, **247**, 429-433.
https://doi.org/10.1016/j.apsusc.2005.01.074

[11] Xie, Q., Deduytsche, D., Schaekers, M., Caymax, M., Delabie, A., Qu, X.-P. and Detavernier, C. (2010) Implementing TiO_2 as Gate Dielectric for Ge-Channel Complementary Metaloxide-Semiconductor Devices by Using HfO_2/GeO_2 Interlayer. *Applied Physics Letters*, **97**, Article ID: 112095. https://doi.org/10.1063/1.3490710

[12] Campbell, S.A., Gilmer, D.C., Wang, X.-C., Hsieh, M.-T., Kim, H.-S., Gladfelter, W.L. and Yan, J. (1997) MOSFET Transistors Fabricated with High Permitivity TiO_2 Dielectrics. *IEEE Transactions on Electron Devices*, **44**, 104-109.
https://doi.org/10.1109/16.554800

[13] Kim, J.Y., Jung, H.S., No, J.H., Kim, J.-R. and Hong, K.S. (2006) Influence of Anatase-Rutile Phase Transformation on Dielectric Properties of Sol-Gel Derived TiO_2 Thin Films. *Journal of Electroceramics*, **16**, 447-451.
https://doi.org/10.1007/s10832-006-9895-z

[14] Kubo, W., Murakoshi, K., Kitamura, T., Yoshida, S., Haruki, M., Hanabusa, K., Shirai, H., Wada, Y. and Yanagida, S. (2001) Quasi-Solid-State Dye-Sensitized TiO_2

Solar Cells: Effective Charge Transport in Mesoporous Space Filled with Gel Electrolytes Containing Iodide and Iodine. *Journal of Physical Chemistry B*, **105**, 12809-12815. https://doi.org/10.1021/jp012026y

[15] Anderson, M.A., Gieselmann, M.J. and Xu, Q. (1988) Titania and Alumina Ceramic Membranes. *Journal of Membrane Science*, **39**, 243-258. https://doi.org/10.1016/S0376-7388(00)80932-1

[16] Wicaksana, D., Kobayashi, A. and Kinbara, A. (1992) Process Effects on Structural Properties of TiO_2 Thin Films by Reactive Sputtering. *Journal of Vacuum Science & Technology A*, **10**, 1479-1482. https://doi.org/10.1116/1.578269

[17] Li, D., Haneda, H., Hishita, S. and Ohashi, N. (2005) Visible-Light-Driven N-F-Codoped TiO_2 Photocatalysts. 1. Synthesis by Spray Pyrolysis and Surface Characterization. *Chemistry of Materials*, **17**, 2588-2595. https://doi.org/10.1021/cm049100k

[18] Djaoued, Y., Badilescu, S., Ashrit, P.V., Bersani, D., Lottici, P.P. and Bruning, R. (2002) Low Temperature Sol-Gel Preparation of Nanocrystalline TiO_2 Thin Films. *Journal of Sol-Gel Science and Technology*, **24**, 247-254. https://doi.org/10.1023/A:1015305328932

[19] Lee, D.H., Cho, Y.S., Yi, W.I., Kim, T.S., Lee, J.K. and Jung, H.J. (1995) Metalorganic Chemical Vapor Deposition of TiO_2:N Anatase Thin Film on Si Substrate. *Applied Physics Letters*, **66**, 815-816. https://doi.org/10.1063/1.113430

[20] Luca, D., Macovei, D. and Teodorescu, C.-M. (2006) Characterization of Titania Thin Films Prepared by Reactive Pulsed-Laser Ablation. *Surface Science*, **600**, 4342-4346. https://doi.org/10.1016/j.susc.2006.01.162

[21] Gÿorgy, E., Del Pino, A.P., Sauthier, G., Figueras, A., Alsina, F. and Pascual, J. (2007) Structural, Morphological and Local Electric Properties of TiO_2 Thin Films Grown by Pulsed Laser Deposition. *Journal of Physics D: Applied Physics*, **40**, 5246-5251. https://doi.org/10.1088/0022-3727/40/17/035

[22] Hsieh, C.C., Wu, K.H., Juang, J.Y., Uen, T.M., Lin, J.Y. and Gou, Y.S. (2002) Monophasic TiO_2 Films Deposited on $SrTiO_3$ (100) by Pulsed Laser Ablation. *Journal of Applied Physics*, **92**, 2518-2523. https://doi.org/10.1063/1.1499522

[23] Ohshima, T., Nakashima, S., Ueda, T., Kawasaki, H., Suda, Y. and Ebihara, K. (2006) Laser Ablated Plasma Plume Characteristics for Photocatalyst TiO_2 Thin Films Preparation. *Thin Solid Films*, **506**, 106-110. https://doi.org/10.1016/j.tsf.2005.08.042

[24] Dzibrou, D., Grishin, A.M. and Kawasaki, H. (2008) Pulsed Laser Deposited TiO_2 Films: Tailoring Optical Properties. *Thin Solid Films*, **516**, 8697-8701. https://doi.org/10.1016/j.tsf.2008.05.010

[25] Long, H., Yang, G., Chen, A., Li, Y. and Lu, P. (2008) Growth and Characteristics of Laser Deposited Anatase and Rutile TiO_2 Films on Si substrates. *Thin Solid Films*, **517**, 745-749. https://doi.org/10.1016/j.tsf.2008.08.179

[26] Kitazawa, S.-I., Choi, Y., Yamamoto, S. and Yamaki, T. (2006) Rutile and Anatase Mixed Crystal TiO_2 Thin Films Prepared by Pulsed Laser Deposition. *Thin Solid Films*, **515**, 1901-1904. https://doi.org/10.1016/j.tsf.2006.07.032

[27] Le Boulbar, E., Millon, E., Boulmer-Leborgne, C., Cachoncinlle, C., Hakim, B. and Ntsoenzok, E. (2014) Optical Properties of Rare Earth-Doped TiO_2 Anatase and Rutile Thin Films Grown by Pulsed-Laser Deposition. *Thin Solid Films*, **553**, 13-16. https://doi.org/10.1016/j.tsf.2013.11.032

[28] Choi, Y., Yamamoto, S., Umebayashi, T. and Yoshikawa, M. (2004) Fabrication and

Characterization of Anatase TiO_2 Thin Film on Glass Substrate Grown by Pulsed Laser Deposition. *Solid State Ionics*, **172**, 105-108. https://doi.org/10.1016/j.ssi.2004.03.014

[29] Janisch, R., Gopal, P. and Spaldin, N.A. (2005) Transition Metal-Doped TiO_2 and ZnO-Present Status of the Field. *Journal of Physics: Condensed Matter*, **17**, R657-R689. https://doi.org/10.1088/0953-8984/17/27/R01

[30] Murugesan, S., Kuppusami, P., Parvathavarthini, N. and Mohandas, E. (2007) Pulsed Laser Deposition of Anatase and Rutile TiO_2 Thin Films. *Surface and Coatings Technology*, **201**, 7713-7719. https://doi.org/10.1016/j.surfcoat.2007.03.004

[31] Djerdj, I. and Tonejc, A.M. (2006) Structural Investigations of Nanocrystalline TiO_2 Samples. *Journal of Alloys and Compounds*, **413**, 159-174. https://doi.org/10.1016/j.jallcom.2005.02.105

[32] Fukuda, K., Fujii, I. and Kitoh, R. (1993) Molecular Dynamics Study of the TiO_2 (Rutile) and TiO_2-ZrO_2 Systems. *Acta Crystallographica B*, **49**, 781-783. https://doi.org/10.1107/S010876819300093X

[33] Di Paola, A., Bellardita, M. and Palmisano, L. (2013) Brookite, the Least Known TiO_2 Photocatalyst. *Catalysts*, **3**, 36-73. https://doi.org/10.3390/catal3010036

[34] Hu, W., Li, L., Li, G., Tang, C. and Sun, L. (2009) High-Quality Brookite TiO_2 Flowers: Synthesis, Characterization, and Dielectric Performance. *Crystal Growth and Design*, **9**, 3676-3682. https://doi.org/10.1021/cg9004032

[35] Moridi, A., Ruan, H., Zhang, L.C. and Liu, M. (2013) Residual Stresses in Thin Film Systems: Effects of Lattice Mismatch, Thermal Mismatch and Interface Dislocations. *International Journal of Solids and Structures*, **50**, 3562-3569. https://doi.org/10.1016/j.ijsolstr.2013.06.022

[36] Gorbenko, O.Y., Samoilenkov, S.V., Graboy, I.E. and Kaul, A.R. (2002) Epitaxial Stabilization of Oxides in Thin Films. *Chemistry of Materials*, **14**, 4026-4043. https://doi.org/10.1021/cm021111v

[37] Dobrovinskaya, E.R., Lytvynov, L.A. and Pishchik, V. (2009) Sapphire: Material, Manufacturing, Applications. Springer Science & Business Media, New York.

[38] Reeber, R.R. and Wang, K. (2000) Lattice Parameters and Thermal Expansion of Important Semiconductors and Their Substrates. *Symposium T—Wide-Bandgap Electronic Devices*, **622**, T6.35.1-T6.35.6.

[39] Blakemore, J.S. (1982) Semiconducting and Other Major Properties of Gallium Arsenide. *Journal of Applied Physics*, **53**, R123-R181. https://doi.org/10.1063/1.331665

[40] Howard, C.J., Kennedy, B.J. and Chakoumakos, B.C. (2000) Neutron Powder Diffraction Study of Rhombohedral Rare-Earth Aluminates and the Rhombohedral to Cubic Phase Transition. *Journal of Physics: Condensed Matter*, **12**, 349-365. https://doi.org/10.1088/0953-8984/12/4/301

[41] Kawamura, K., Yashima, M., Fujii, K., Omoto, K., Hibino, K., Yamada, S., Hester, J.R., Avdeev, M., Miao, P., Torii, S. and Kamiyama, T. (2015) Structural Origin of the Anisotropic and Isotropic Thermal Expansion of K2NiF4-Type $LaSrAlO_4$ and Sr2TiO4. *Inorganic Chemistry*, **54**, 3896-3904. https://doi.org/10.1021/acs.inorgchem.5b00102

[42] Hössinger, A. (2000) Simulation of Ion Implantation for ULSI Technology. PhD Dissertation, Vienna University of Technology, Wien.

[43] Watanabe, H., Yamada, N. and Okaji, M. (2004) Linear Thermal Expansion Coefficient of Silicon from 293 to 1000 K. *International Journal of Thermophysics*, **25**, 221-236. https://doi.org/10.1023/B:IJOT.0000022336.83719.43

[44] Ackermann, R.J. and Sorrell, C.A. (1974) Thermal Expansion and the High-Low Transformation in Quartz. I. High-Temperature X-Ray Studies. *Journal of Applied Crystallography*, **7**, 461-467. https://doi.org/10.1107/S0021889874010211

[45] Schmidbauer, M., Kwasniewski, A. and Schwarzkopf, J. (2012) High-Precision Absolute Lattice Parameter Determination of $SrTiO_3$, DyScO3 and NdGaO3 Single Crystals. *Acta Crystallographica B*, **68**, 8-14. https://doi.org/10.1107/S0108768111046738

[46] de Ligny, D. and Richet, P. (1996) High-Temperature Heat Capacity and Thermal Expansion of $SrTiO_3$ and $SrZrO_3$ Perovskites. *Physical Review B*, **53**, 3013-3022. https://doi.org/10.1103/PhysRevB.53.3013

[47] Wood, R.M. (1962) The Lattice Constants of High Purity Alpha Titanium. *Proceedings of the Royal Society A*: *Mathematical, Physical and Engineering Sciences*, **80**, 783-787.

[48] Spreadborough, J. and Christian, J.W. (1959) The Measurement of the Lattice Expansion of Debye Temperatures of Titanium and Silver by X-Ray Methods. *Proceedings of the Physical Society*, **74**, 609-615. https://doi.org/10.1088/0370-1328/74/5/314

[49] Kawasaki, M., Takahashi, K., Maeda, T., Tsuchiya, R., Shinhara, M., Ishiyama, O., Yonezawa, T., Yoshimoto, M. and Koinuma, H. (1994) Atomic Control of the $SrTiO_3$ Crystal Surface. *Science*, **266**, 1540-1542. https://doi.org/10.1126/science.266.5190.1540

[50] Koster, G., Kropman, B.L., Rijnders, G.J.H.M., Blank, D.H.A. and Rogalla, H. (1998) Quasi-Ideal Strontium Titanate Crystal Surfaces through Formation of Strontium Hydroxide. *Applied Physics Letters*, **73**, 2920-2922. https://doi.org/10.1063/1.122630

[51] Kennedy, R.J. and Stampe, P.A. (2003) The Influence of Lattice Mismatch and Film Thickness on the Growth of TiO_2 on $LaAlO_3$ and $SrTiO_3$ Substrates. *Journal of Crystal Growth*, **252**, 333-342. https://doi.org/10.1016/S0022-0248(02)02514-9

[52] Luo, Y.-R. (2007) Comprehensive Handbook of Chemical Bond Energies. CRC Press, Boca Raton. https://doi.org/10.1201/9781420007282

[53] Gouma, P.I. and Mills, M.J. (2001) Anatase-to-Rutile Transformation in Titania Powders. *Journal of the American Ceramic Society*, **84**, 619-622. https://doi.org/10.1111/j.1151-2916.2001.tb00709.x